Polym. Bull. (2012) 68:561–573
DOI 10.1007/s00289-011-0651-4

ORIGINAL PAPER

Electromagnetic interference shielding effects of polyaniline-coated multi-wall carbon nanotubes/maghemite nanocomposites

Jumi Yun · Hyung-Il Kim

Received: 27 April 2011 / Revised: 4 August 2011 / Accepted: 7 October 2011 /
Published online: 15 October 2011

Abstract Highly conductive nanocomposites were prepared by in situ polymerization of polyaniline (PANi) and multi-walled carbon nanotubes (MWCNTs) as electromagnetic interference shielding materials. γ-Fe_2O_3 nanoparticles were also incorporated in the nanocomposites to improve the ferromagnetic properties. SEM and TEM images showed the uniformly coated PANi on the surface of MWCNTs and γ-Fe_2O_3. XRD peaks also confirmed the presence of MWCNT and γ-Fe_2O_3 in the nanocomposites. The nanocomposites showed significant improvement in permittivity, permeability, and electromagnetic interference shielding efficiency due to the conductive effect of MWCNTs and the magnetic effect of γ-Fe_2O_3. The electromagnetic interference shielding efficiency of nanocomposites increased up to 34.1 dB due to the synergetic effect of reflection and absorption of electromagnetic interference by MWCNTs and γ-Fe_2O_3 additives.

Keywords Electromagnetic interference shielding · Polyaniline · Carbon nanotubes · Maghemite · Nanocomposite

Introduction

The proliferation of electronics and instrumentation in commercial, industrial, healthcare, and defense sectors has led to new pollution known as electromagnetic interference (EMI) [1]. It is caused by the interference effects induced by electric and magnetic fields, emanating from wide range of electrical circuitry [2]. The interference among business machines, process equipments, consumer products, and other instruments may lead to either disturbance of normal performance or complete

J. Yun · H.-I. Kim (✉)
Department of Fine Chemical Engineering and Applied Chemistry, BK21-E2M, Chungnam National University, Daejeon 305-764, Republic of Korea
e-mail: hikim@cnu.ac.kr

malfunction. The disturbances across communication channels, automation, and process control may lead to loss of time, energy, resources, and human health. Therefore, the EMI shielding materials are studied extensively. Although metals were the most common materials for EMI shielding traditionally, their disadvantages include high density, susceptibility to corrosion, complex, and uneconomic processing [3, 4].

Polymer/inorganic nanocomposites have attracted the attention as EMI shielding materials due to the combined nature of flexibilities, improved processability of polymers, high modulus, transparency, surface hardness, and heat resistance [5]. The composites of conducting polymer containing magnetic nanoparticles have attracted interests due to the unique combination of magnetic, electric, and optical properties. They have many potential applications in EMI shielding, electrochromic device, and non-linear optical system [6–8]. Among various conducting polymers, polyaniline (PANi) has been regarded as the candidate for EMI shielding because of its various structures, special doping mechanism, excellent environmental stability, favorable solution processability, and wide applications as electronic materials [9, 10]. Among inorganic nanoparticles, iron oxides have received great attention as EMI shielding materials due to the magnetic properties as well as extensive applications such as color imaging, recording media, and ferrofluids.

Carbon nanotubes (CNTs) also attract the increased attention from material scientists. CNTs have been used to improve the mechanical and thermal properties of composites. CNTs also impart the electrical conductivity to the composite even at lower content, which is an important factor in the composites for EMI shielding. The difficulty in using CNTs as conductive additive is the poor dispersion of CNTs in composite, resulting in the interior electric and mechanical properties [11–13].

In this study, highly conductive PANi and multi-walled carbon nanotubes (MWCNTs) nanocomposites were prepared by in situ polymerization for electromagnetic interference shielding. γ-Fe_2O_3 nanoparticles were incorporated to improve the ferromagnetic properties of the nanocomposites. The surface treatment of MWCNTs was carried out using oxyfluorination to improve the dispersion of MWCNTs in the composite based on previous works [14]. The synergetic effects of using these magnetic and conductive ingredients were investigated based on morphology and EMI shielding behavior.

Experimental

Materials

Aniline, ammonium persulfate (APS), and hydrochloride (HCl) were obtained from Aldrich. Aniline was distilled in vacuum before use. γ-Fe_2O_3 (<50 nm, Aldrich) and MWCNTs (average diameter: 20–50 nm, Aldrich) were used as functional additives for nanocomposites.

Preparation of PANi/MWCNT/γ-Fe_2O_3 nanocomposites

Oxyfluorination of MWCNT was carried out to modify the surface properties of MWCNTs. Oxyfluorination was carried out at 1 bar for 3 min with the oxygen to

fluorine gas ratio of 8:2. The hydrophobic surface of MWCNTs was modified to carry the hydrophilic functional groups by oxyfluorination resulting in the improved dispersion of MWCNTs in hydrophilic media. PANi/MWCNT/γ-Fe_2O_3 nanocomposites were prepared by the oxidation of aniline hydrochloride dissolved in ethanol with an aqueous solution of ammonium peroxide in the presence of oxyfluorinated MWCNTs and γ-Fe_2O_3. In typical synthetic process, equal volumes of HCl solutions containing 5 wt% oxyfluorinated MWCNTs, γ-Fe_2O_3, and aniline monomer were sonicated for 2 h to form the uniform suspensions. APS dissolved in HCl solution was added slowly into the aniline solution to initiate the polymerization. The reaction mixture was reacted for 6 h at 4 °C with stirring to have aniline fully polymerized. The synthesized PANi/MWCNT/γ-Fe_2O_3 nanocomposites were filtered and rinsed several times with distilled water, acetone, and methanol, respectively. Various nanocomposites are classified in Table 1.

Characterization

Field emission scanning electron microscopy (FE-SEM, Hitachi, S-5500) was used to investigate the surface morphology. Images were taken without prior treatment to ensure the acquisition of accurate images. The diameter of nanofiber and the size of cluster were measured by the software program installed in the FE-SEM. The morphology of nanocomposites was also examined using field emission transmission electron microscopy (FE-TEM, Tecnai G^2 F30 S-TWIN). FE-TEM samples were prepared by dispersing the nanocomposites in isopropanol under sonication and placing small drops of suspension on the carbon-coated copper grids.

The presence of MWCNT and γ-Fe_2O_3 in nanocomposite was confirmed by X-ray diffraction (XRD, Rigaku, D/MAX-2200 Ultima/PC) in scattering range (2θ) of 10°–60° with a scan rate of 0.02° s^{-1} and slit width of 0.1 mm.

The magnetic measurements of the samples were performed using the vibrating sample magnetometer (VSM, Lakeshore Cryotronics, model 7304) with a maximum magnetic field of 1.2 T. The sample was placed in Perspex sample holder which was vibrated horizontally with the frequency of 76 Hz.

The electrical conductivity of the samples was measured using a four-probe method. The samples for measuring the resistance were prepared by applying pressure of 1000 psi without any binder. The sample was pellet type with about 10 mm in diameter and 2 mm in thickness. The pellet type samples were cemented with silver paint to Pt leads which were printed on an alumina plate to avoid the contact resistance. The resistance was measured three times with a four-probe

Table 1 Classification of PANi/MWCNT/γ-Fe_2O_3 nanocomposites

Abbreviation	Compositions		
	Aniline	γ-Fe_2O_3	MWCNT
PANi	O	–	–
PF	O	O	–
PC	O	–	O
PCF	O	O	O

method at room temperature with the probe head station and the ASTM F1529-97 method. The electrical conductivity (σ) was calculated using the following equations [15]:

$$\rho = \mathrm{Rs} \times t\ (\Omega\ \mathrm{cm})$$

$$\sigma = 1/\rho\ (\mathrm{S/cm})$$

where ρ and t are the bulk resistivity and the thickness of sample, respectively.

Permittivity, magnetic permeability, and EMI shielding efficiency (SE) were obtained according to the ASTM D-4935-99 method using a network analyzer (Agilent, E5071A) equipped with an amplifier and a scattering parameter (S-parameter) test set over the frequency range of 800 MHz–2.5 GHz. Annular disks were prepared with a punching machine and installed into a test tool as depicted in previous work [15]. EMI SE was calculated using S parameters with the equations found in the literatures [16–18].

Results and discussion

Morphology

Figures 1a and 2a show SEM and TEM images of PANi prepared from aniline solutions. The formation of self-assembled micelle structure of PANi was suggested for the aniline polymerization with acidic dopant by several researchers [19–21] and it was confirmed by Fig. 1a, b. Figure 1b illustrates the PANi-coated MWCNTs of core–shell morphology. The uniform deposition of PANi on the surface of MWCNTs is also confirmed by TEM in Fig. 2b. Aniline could be easily adsorbed on the surface-modified MWCNTs resulting in the template polymerization [22]. The formation of PC nanocomposite is represented schematically in Scheme 1a.

PF nanocomposites were prepared by in situ polymerization to reduce the agglomeration of γ-Fe_2O_3 nanoparticles. The color of reactant solution changed to green upon polymerization of aniline in the presence of γ-Fe_2O_3. γ-Fe_2O_3 nanocomposites showed the morphology of uniformly dispersed γ-Fe_2O_3 nanoparticles in PANi as shown in Fig. 2c, d. The formations of PF and PCF nanocomposites are represented schematically in Scheme 1b, c, respectively. PF and PCF nanocomposites were found to show the magnetic response in the applied magnetic field. Therefore, these nanocomposites could be separated from the suspension by magnet.

X-ray diffraction analysis

XRD studies were carried out to identify γ-Fe_2O_3 and MWCNT in the nanocomposites as shown in Fig. 3. PF and PCF nanocomposites showed the γ-Fe_2O_3 peaks clearly demonstrating that the structural changes did not occur in γ-Fe_2O_3 during in situ polymerization. XRD peak at 26.5° is attributed to the graphite-structured carbons (002) of MWCNTs. PANi also showed the peak at 26.5° indicating the aromatic carbon rings.

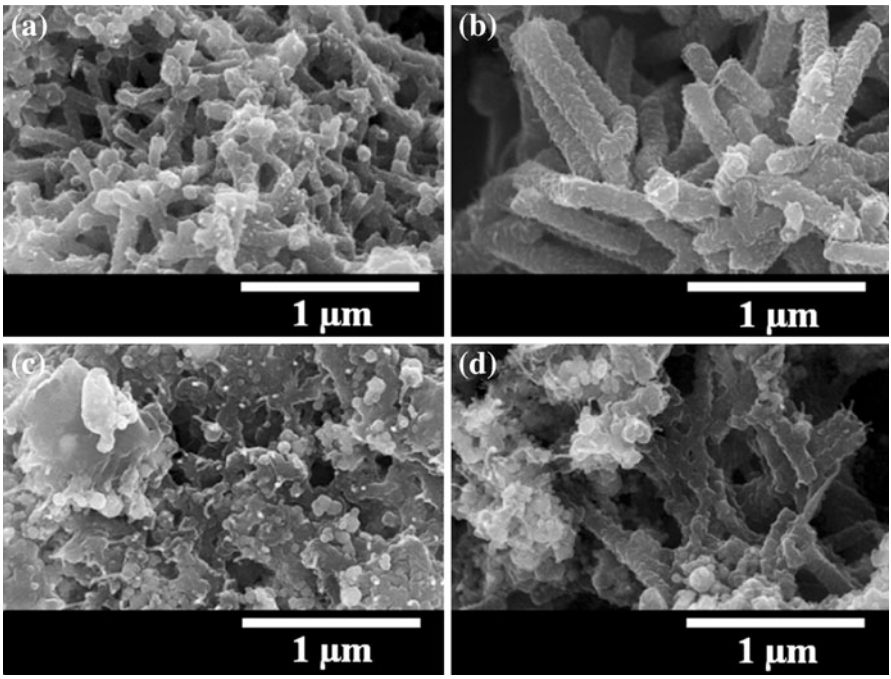

Fig. 1 SEM images of various nanocomposites: **a** PANi, **b** PC, **c** PF, and **d** PCF

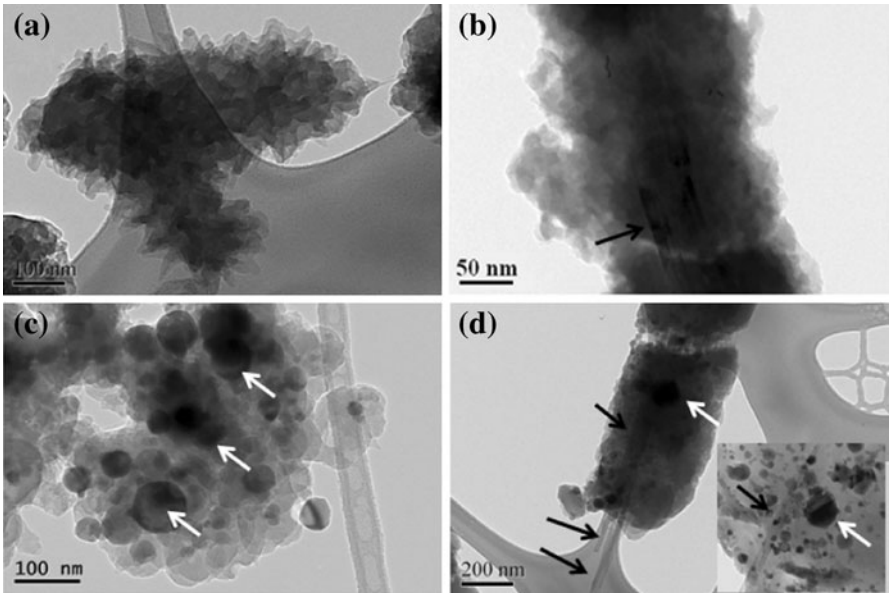

Fig. 2 Morphologies of **a** PANi, **b** PC, **c** PF, and **d** PCF observed by TEM. *Black* and *white* arrows indicate MWCNT and γ-Fe_2O_3, respectively

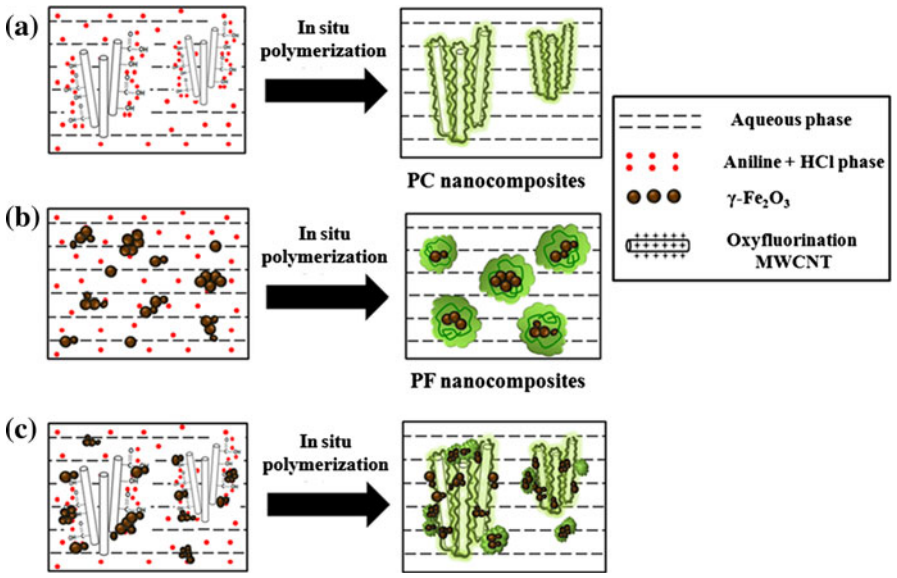

Scheme 1 Schematic representation of formation of PC, PF, and PCF nanocomposites

Electrical and magnetic properties

Electrical and magnetic properties of nanocomposites are shown in Table 2 and Fig. 4. When PANi was coated on MWCNTs, the conductivity increased considerably from 3.08 to 15.39 S/cm. The improved conductivity of nanocomposites is mainly due to the effective combination of the intrinsic conductivities of MWCNT and PANi [23, 24]. The conductivity of MWCNT pellets is usually much lower than the intrinsic conductivity of the MWCNTs because the pellets of non-coated MWCNTs contain mechanically disordered and entangled MWCNT masses in which individual tubes are not packed efficiently to maximize the intertube contact area. Intertube contact area of non-coated MWCNTs is probably small because MWCNTs resist the deformation under compression due to higher mechanical strength [24]. PANi-coating on MWCNTs is favorable in increasing the intertube contact area due to the increased tube diameter and the relatively softer PANi phase. Entanglements among PANi chains on the surface of contacting MWCNTs may also shorten the circuit intertube tunneling pathways, providing the conductive polymer paths bridging [24]. The decrease in conductivity of γ-Fe_2O_3-contained nanocomposites is due to the decrease in the proton doping level and blockage of conducting path by the γ-Fe_2O_3 embedded in the PANi matrix.

The effect of γ-Fe_2O_3 addition on the magnetization of nanocomposites was investigated and variations in saturated magnetization (Ms) and coercive force (Hc) are presented in Fig. 4 and Table 2. Pristine γ-Fe_2O_3 had Ms of 21.1 emu/g and Hc of 169 Oe, respectively. PF and PCF showed the obvious magnetic properties

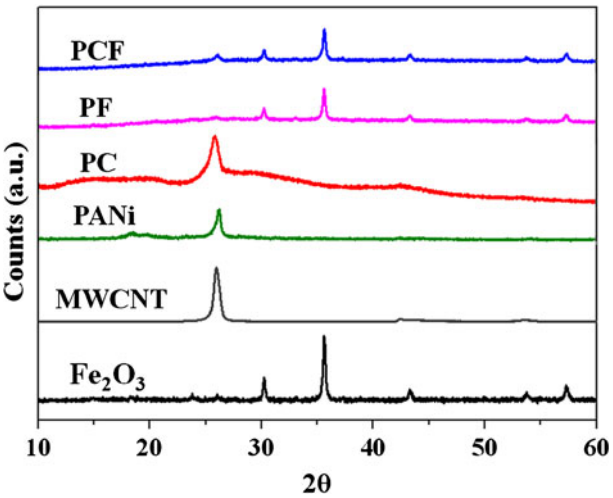

Fig. 3 XRD patterns of various nanocomposites

Table 2 Electrical and magnetic properties of nanocomposites

Sample	Conductivity (S/cm)	Ms (emu/g)	Hc (Oe)
γ-Fe_2O_3	–	21.1	169.0
PANi	3.08	–	–
PF	1.98	19.3	149.0
PC	15.39	–	–
PCF	12.55	15.0	115.5
MWCNT	10.12	–	–

Ms saturated magnetization

Hc coercive force

although both Ms and Hc decreased somewhat due to the dilution effect. *M–H* hysteresis loops were investigated for PF and PCF. Open-loop hysteresis was observed for both PF and PCF, indicating the presence of well-dispersed superparamagnetic nanoparticles in the nanocomposites [25–27]. The magnetization property of PANi was too small to sense the effect of applied magnetic field. This result is correlated well with the results presented by other groups [28, 29].

Thermal stability

The effect of MWCNTs and γ-Fe_2O_3 on the thermal stability of nanocomposites was studied as shown in Fig. 5. The evaporation of moisture adsorbed on the nanocomposites is observed below 100 °C. Major degradation of PANi occurred below 200 °C [30]. However, the degradation rate decreased significantly by incorporating γ-Fe_2O_3 and MWCNT in the nanocomposites indicating the favorable

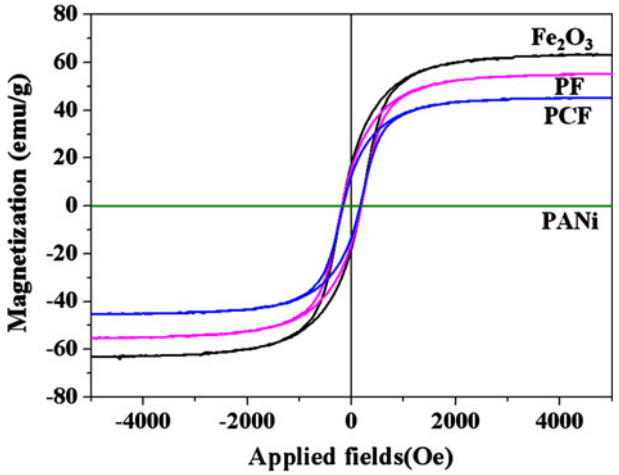

Fig. 4 *M–H* hysteresis loops of PANi, γ-Fe_2O_3, PF, and PCF nanocomposites at room temperature

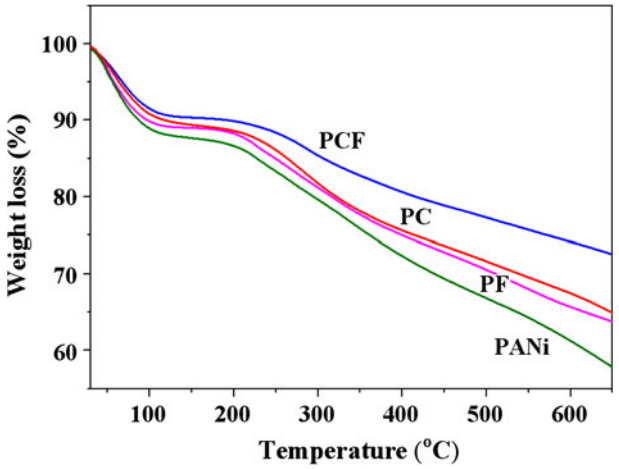

Fig. 5 TGA thermograms of various nanocomposites

interactions with PANi. The adsorption of free radicals generated during degradation on MWCNTs could also contribute to the thermal stability in some extent [31].

EMI shielding characteristics

The permittivities of nanocomposites are shown in Fig. 6. The real (ε_r) and imaginary permittivities (ε_i) increased mainly by incorporating MWCNTs in the nanocomposites. The permittivity of PC increased more than twice compared with that of PANi due to the high electrical conductivity of MWCNTs [32–35].

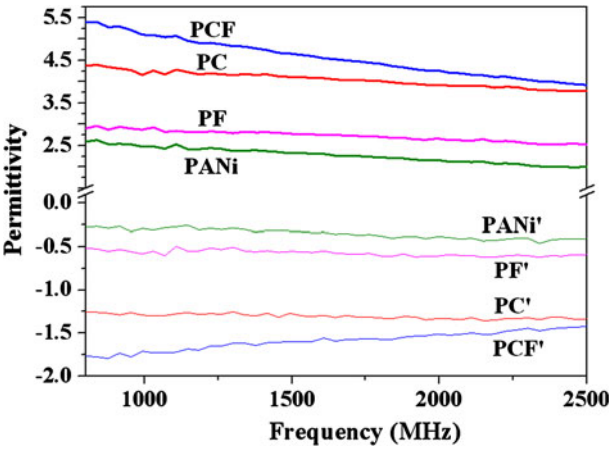

Fig. 6 Permittivities of PANi, PF, PC, and PCF nanocomposites

The permeabilities of nanocomposites are presented in Fig. 7. The permeability increased significantly for the nanocomposites containing γ-Fe_2O_3 which has excellent magnetic property.

EMI SEs of nanocomposites are presented in Fig. 8. EMI SE of nanocomposites increased noticeably due to the contributions of higher permittivity of MWCNTs and higher permeability of γ-Fe_2O_3, respectively. The contributions of MWCNTs and γ-Fe_2O_3 to EMI SE are represented schematically in Scheme 2. The highly conductive MWCNTs improve EMI SE by decreasing the electrical interference effectively. On the other hand, the magnetic γ-Fe_2O_3 improves EMI SE mainly by decreasing the magnetic interference.

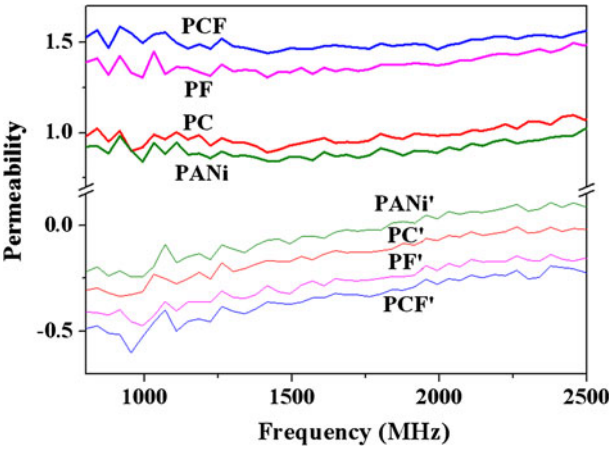

Fig. 7 Permeabilities of PANi, PF, PC, and PCF nanocomposites

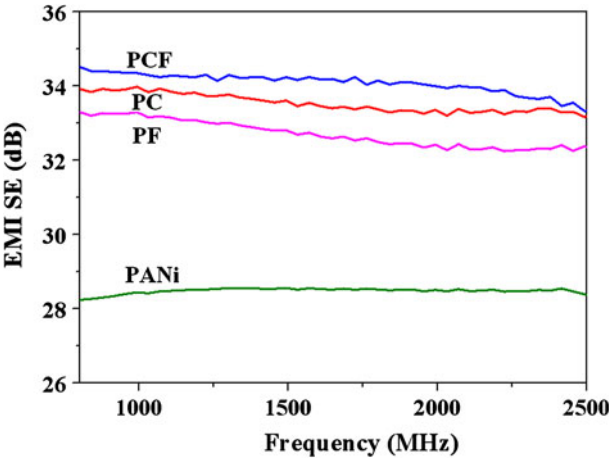

Fig. 8 EMI SE of PANi, PF, PC, and PCF nanocomposites

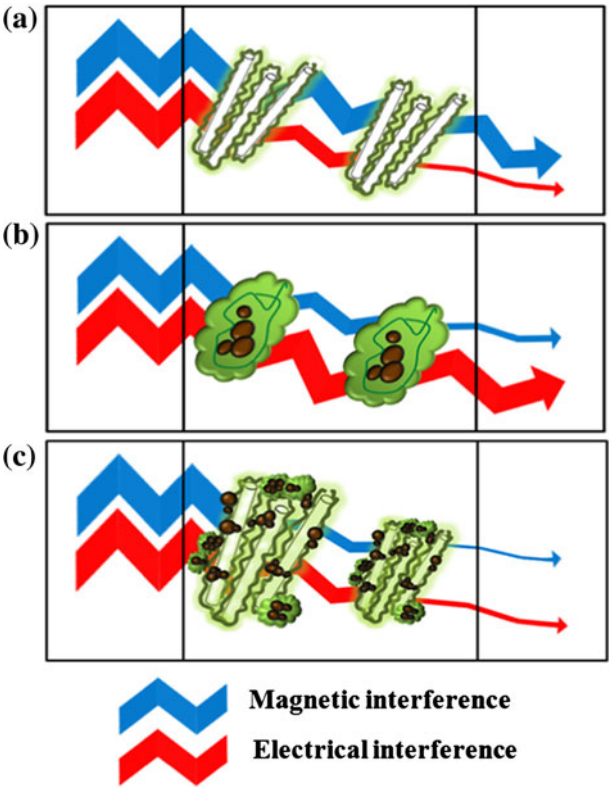

Scheme 2 Schematic representation of EMI shielding contribution by MWCNTs and γ-Fe_2O_3: **a** PC, **b** PF, and **c** PCF

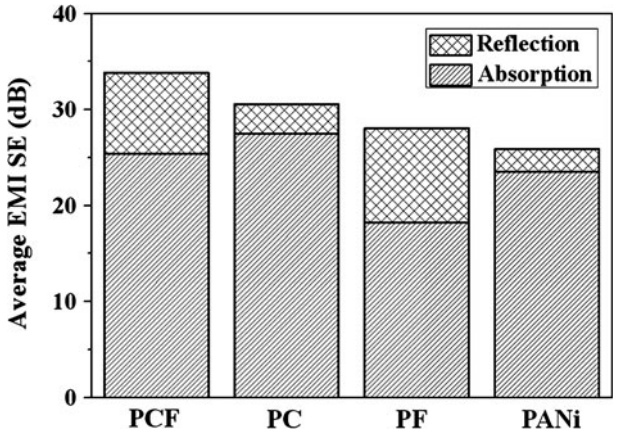

Fig. 9 Average EMI SE of various nanocomposites by reflection and adsorption effects

EMI is generally shielded by reflection and absorption mechanisms [32]. EMI SEs of various nanocomposites are specified by reflection and absorption in Fig. 9. EMI SE is defined as following equations [32].

$$\text{EMI SE}_\text{T} = \text{EMI SE}_\text{R} + \text{EMI SE}_\text{A}$$

$$\text{EMI SE}_\text{R} = 20\log(\eta_0/4\eta_\text{s})$$

EMI SE_R and EMI SE_A stand for the EMI SE by reflection and absorption effects, respectively. η_0 is propagating domain and η_s is intrinsic impedance of the shielding material. EMI was shielded mainly by reflection for the γ-Fe_2O_3-contained nanocomposites. However, the main mechanism of EMI shielding changed into absorption for the MWCNTs-contained nanocomposites. Therefore, the use of both MWCNTs and γ-Fe_2O_3 together might give the synergetic effects in EMI shielding as in the case of PCF.

Conclusions

PANi/MWCNT/γ-Fe_2O_3 nanocomposites were prepared by in situ polymerization. PANi was coated uniformly on the surface of MWCNT/γ-Fe_2O_3 as confirmed from the morphology investigated with SEM and TEM. The prepared nanocomposites showed the significant improvement in permittivity, permeability, and electromagnetic interference SE due to the magnetic effects of γ-Fe_2O_3 and the conductive effect of MWCNTs. EMI SE increased from 28.2 to 34.1 dB by incorporating MWCNT and γ-Fe_2O_3 in PANi. These additives contributed a large share to the synergetic improvement of EMI SE in both reflection and absorption mechanisms and the thermal stability of nanocomposites. PANi/MWCNT/γ-Fe_2O_3 nanocomposites could be applied as the hybrid conductive additives in various polymer matrices as efficient EMI shielding materials.

Acknowledgment This research was financially supported by the Ministry of Education, Science Technology (MEST) and Korea Institute for Advancement of Technology (KIAT) through the Human Resource Training Project for Regional Innovation.

References

1. Olmedo L, Hourquebie P, Jousse F (1997) Handbook of organic conductive molecules and polymers. John Wiley and Sons, Chichester
2. Im JS, Kim JG, Lee SH, Lee YS (2010) Effective electromagnetic interference shielding by electrospun carbon fibers involving Fe_2O_3/$BaTiO_3$/MWCNT additives. Mater Chem Phys 124:434–438
3. Liang J, Wang Y, Huang Y, Ma Y, Liu Z, Cai J (2009) Electromagnetic interference shielding of grapheme/epoxy composites. Carbon 47:922–925
4. Fugetsu B, Sano E, Sunada M, Sambongi Y, Shibuya T, Wang X (2008) Electrical conductivity and electromagnetic interference shielding efficiency of carbon nanotube/cellulose composite paper. Carbon 46:1256–1258
5. Novak BM (1993) Hybrid nanocomposite materials—between inorganic glasses and organic polymers. Adv Mater 5:422–433
6. Miyauchi S, Aiko H, Sorimashi Y, Tsubats I (1989) Preparation of barium titanate-polypyrrole compositions and their electrical properties. J Appl Polym Sci 37:289–293
7. Shen PK, Huang HT, Tseung ACC (1992) A study of tungsten trioxide and polyaniline composite films. J Electrochem Soc 139:1840–1845
8. Peng X, Zhang Y, Yang J, Zou B, Xia PL (1992) Formation of nanoparticulate iron(III) oxide-stearate multilayer through Langmuir-Blodgett method. J Phys Chem 96:3412–3415
9. Tai H, Jiang Y, Xie G, Yu J (2010) Preparation, characterization and comparative NH3-sensing characteristic studies of PANI/inorganic oxides nanocomposite thin films. J Mater Sci Technol 26:605–613
10. Jansen SA, Duong T, Major A, Wei Y, Sein LT Jr (1999) Evolution of the electronic states of polyaniline: an ab initio analysis of the orbital states of PAni synthons. Synth Met 105:107–113
11. Spitalsky Z, Tasis D, Papagelis K, Galiotis C (2010) Carbon nanotube-polymer composites: chemistry, processing, mechanical and electrical properties. Prog Polym Sci 35:357–401
12. Wu TM, Chang HL, Lin YW (2009) Synthesis and characterization of conductive polypyrrole/multiwalled carbon nanotubes composites with improved solubility and conductivity. Compos Sci Technol 69:639–644
13. Ratna D, Abraham TN, Siengchin S, Karger-Kocsis J (2009) Novel method for dispersion of multiwall carbon nanotubes in poly(ethylene oxide) matrix using dicarboxylic acid salts. J Polym Sci B Polym Phys 47:1156–1165
14. Yun J, Im JS, Lee YS, Kim HI (2010) Effect of oxyfluorination on electromagnetic interference shielding behavior of MWCNT/PVA/PAAc composite microcapsules. Eur Polym J 46:900–909
15. Wu Z, Li J, Timmer D, Lozano K, Bose S (1970) Study of processing variables on the electrical resistivity of conductive adhesives. Int J Adhes Adhes 29:488–494
16. Nicolson AM, Ross GF (1970) Measurement of the intrinsic properties of materials by time-domain techniques. IEEE Trans Instrum Meas 19:377–382
17. Ghodgaonkar DK, Vardan VV, Varadan VK (1990) Free-space measurement of complex permittivity and complex permeability of magnetic materials at microwave frequencies. IEEE Trans Instrum Meas 39:387–394
18. Hong YK, Lee CY, Jeong CK, Lee DE, Kim K, Joo J (2003) Method and apparatus to measure electromagnetic interference shielding efficiency and its shielding characteristics in broadband frequency ranges. Rev Sci Instrum 74:1098–1102
19. Zhang L, Wan M (2002) Synthesis and characterization of self-assembled polyaniline nanotubes doped with D-10-camphorsulfonic acid. Nanotechnology 13:750–755
20. Kim BJ, Oh SG, Han MG, Im SS (2000) Preparation of polyaniline nanoparticles in micellar solutions as polymerization medium. Langmuir 16:5841–5845
21. Harada M, Adachi M (2000) Surfactant-mediated fabrication of silica nanotubes. Adv Mater 12:839–841
22. Stejskal J, Sapurina I (2005) Polyaniline: thin films and colloidal dispersions. Pure Appl Chem 77:815–826

23. Ruschau GR, Yoshikawa S, Newnham RE (1992) Resistivities of conductive composites. J Appl Phys 72:953–959
24. Makeiff DA, Huber T (2006) Microwave absorption by polyaniline-carbon nanotube composites. Synth Met 156:497–505
25. Zhongzhu W, Hong B, Jian L, Tao S, Xianliang W (2008) Magnetic and microwave absorbing properties of polyaniline/γ-Fe2O3 nanocomposite. J Magn Magn Mater 320:2132–2139
26. Alam J, Riaz U, Ahmad S (2007) Effect of ferrofluid concentration on electrical and magnetic properties of the Fe_3O_4/PANI nanocomposites. J Magn Magn Mater 314:93–99
27. Yunze L, Zhaojia C, Jean LD, Zhiming Z, Meixiang W (2005) Electrical and magnetic properties of polyaniline/Fe_3O_4 nanostructures. Physica B 370:121–130
28. Shengqi L, Chunxia Z, Li T, Jinqing K (2010) Unique properties of polyaniline in the presence of applied magnetic field and ferric chloride. Mater Chem Phys 124:168–172
29. Zhifu H, Yang F, Xiaojuan W, Hua P (2011) Microwave absorption properties of PANI/CIP/Fe_3O_4 composites. Synth Met 161:420–425
30. Yu Y, Che B, Si Z, Li L, Chen W, Xue G (2005) Carbon nanotube/polyaniline core-shell nanowires prepared by in situ inverse microemulsion. Synth Met 150:271–277
31. Shaffer MSP, Windle AH (1999) Fabrication and characterization of carbon nanotube/poly(vinyl alcohol) composites. Adv Mater 11:937–941
32. Al-Saleh MH, Sundararaj U (2009) Electromagnetic interference shielding mechanisms of CNT/polymer composites. Carbon 47:1738–1746
33. Wang LL, Tay BK, See KY, Sun Z, Tan LK, Lua D (2009) Electromagnetic interference shielding effectiveness of carbon-based materials prepared by screen printing. Carbon 47:1905–1910
34. Im JS, Park IJ, In SJ, Kim T, Lee YS (2009) Fluorination effects of MWCNT additives for EMI shielding efficiency by developed conductive network in epoxy complex. J Fluor Chem 130:1111–1116
35. Lee JM, Kim SJ, Kim JW, Kang PH, Nho YC, Lee YS (2009) A high resolution XPS study of sidewall functionalized MWCNTs by fluorination. J Ind Eng Chem 15:66–71